Supplementary Information

Bioelectrochemistry of Cytochrome *c* in a Closed Bipolar Electrochemical Cell

Alonso Gamero-Quijano,[a] Grégoire Herzog,[b]* Micheál D Scanlon[a,c]*

[a] The Bernal Institute and Department of Chemical Sciences, School of Natural Sciences, University of Limerick (UL), Limerick V94 T9PX, Ireland.

[b] Laboratoire de Chimie Physique et Microbiologie pour les Matériaux et l'Environnement (LCPME), UMR 7564, CNRS, Université de Lorraine, 405 rue de Vandoeuvre, Villers-lès-Nancy, F-54600, France.

[c] Advanced Materials and Bioengineering Research (AMBER) Centre, Ireland.

*Corresponding authors:

gregoire.herzog@univ-lorraine.fr

micheal.scanlon@ul.ie

S1 Supplementary experimental methods

S.1.1 Materials

All chemicals were used as received without further purification. All aqueous solutions were prepared with ultra pure water (Millipore Milli-Q, specific resistivity 18.2 MΩ·cm). The organic solvent α,α,α-trifluorotoluene (TFT, 99+%) was received from Acros Organics. Cytochrome *c* (Cyt *c*) from bovine heart (≥ 95%) was purchased from Sigma-Aldrich. The iron in the heme group of Cyt *c* is in its oxidised form (Cyt *c*-Fe$^{(III)}$). The lipophilic reductants ferrocene (Fc, 98%), dimethylferrocene (DiMFc, 95%) and decamethylferrocene (DcMFc, 97%) were purchased from Sigma-Aldrich. Bis(triphenylphosphoranylidene) ammonium chloride (BACl, 97%), potassium ferricyanide (K$_3$Fe(CN)$_6$, ≥99%), potassium ferrocyanide (K$_4$Fe(CN)$_6$·3H$_2$O, ≥99.95%), tetramethylammonium chloride (TMACl, ≥ 98%), lithium chloride (LiCl, ≥ 95%) and phosphate buffered saline (PBS) tablets were purchased from Sigma-Aldrich. Lithium tetrakis(pentafluorophenyl)borate diethyletherate ([Li(OEt$_2$)$_2$]TB) was received from Boulder Scientific Company.

BACl and [Li(OEt$_2$)$_2$]TB were used to prepare the organic electrolyte salt bis(triphenylphosphoranylidene) ammonium tetrakis(pentafluorophenyl)borate (BATB) by metathesis of equimolar solutions of BACl and [Li(OEt$_2$)]TB in a methanol-water (2:1 v/v) mixture. The resulting precipitates were filtered, washed and recrystallised from acetone. The pH of the aqueous Cyt *c* solutions was fixed to pH 7 by preparing a phosphate buffer solution by dissolving a PBS tablet in ultra pure water and diluting to achieve final concentrations of 2.00 mM phosphate buffer, 0.54 mM potassium chloride (KCl), and 27.40 mM sodium chloride (NaCl).

S.1.2 Calibration of CVs obtained in aqueous phosphate buffer solution with a 3-electrode cell using Ag/AgCl reference electrodes to the SHE scale

The onset potential for the hydrogen evolution reaction in an aqueous phosphate buffer solution at pH 7 is –0.413 V *versus* SHE [1]. Using a 3-electrode cell, the onset potential for the hydrogen evolution reaction in an aqueous phosphate buffer solution at pH 7 (degassed, and maintained under an inert N$_2$ atmosphere) *versus* the aqueous Ag/AgCl reference electrode ($\left[E^{1/2}\right]_{Ag/AgCl}^{w}$) was determined as –0.744 V (Fig. S1(A)). Thus, the offset potential difference

between the aqueous Ag/AgCl reference electrode used herein and the SHE ($\Delta E_{\text{Ag/AgCl } vs. \text{ SHE}}^{\text{w}}$) was 0.331 V, since $\Delta E_{\text{Ag/AgCl } vs. \text{ SHE}}^{\text{w}} = \left(\left[E^{\ominus} \right]_{\text{SHE}}^{\text{w}} - \left[E^{1/2} \right]_{\text{Ag/AgCl}}^{\text{w}} \right)$.

The redox potential of an equimolar solution of $[\text{Fe}^{\text{(III)}}(\text{CN})_6]^{3-}/\text{Fe}^{\text{(II)}}(\text{CN})_6]^{4-}$ redox probes in phosphate buffer solution, with a molar concentration of ~50 mM, at pH 7 *versus* SHE ($\left[E^{\ominus} \right]_{\text{SHE}}^{\text{w}}$) has been determined previously as +0.418 V [2]. As the electrochemistry of ITO in the absence of any redox probes is featureless, this redox probe was used to calibrate the CVs obtained with ITO working electrodes. Using a 3-electrode cell, the half-wave potential of an equimolar solution of $[\text{Fe}^{\text{(III)}}(\text{CN})_6]^{3-}/\text{Fe}^{\text{(II)}}(\text{CN})_6]^{4-}$ in phosphate buffer solution, with a molar concentration of ~30 mM, at pH 7 *versus* the aqueous Ag/AgCl reference electrode ($\left[E^{1/2} \right]_{\text{Ag/AgCl}}^{\text{w}}$) was determined as +0.092 V (Fig. S1(B)). Thus, $\Delta E_{\text{Ag/AgCl } vs. \text{ SHE}}^{\text{w}}$ was 0.326 V. This is in excellent agreement ($\pm$ 5 mV) with the value of $\Delta E_{\text{Ag/AgCl } vs. \text{ SHE}}^{\text{w}}$ determined with the same Ag/AgCl reference electrode using the Pt wire working electrode in Fig. S1(A).

The phosphate buffer solution contained 0.54 mM KCl and 27.40 mM NaCl, and therefore this chloride concentration allowed the potential of the Ag/AgCl wire used herein to remain stable. The stability of the latter was monitored at regular intervals *versus* a Ag/AgCl (3 M KCl) reference electrode.
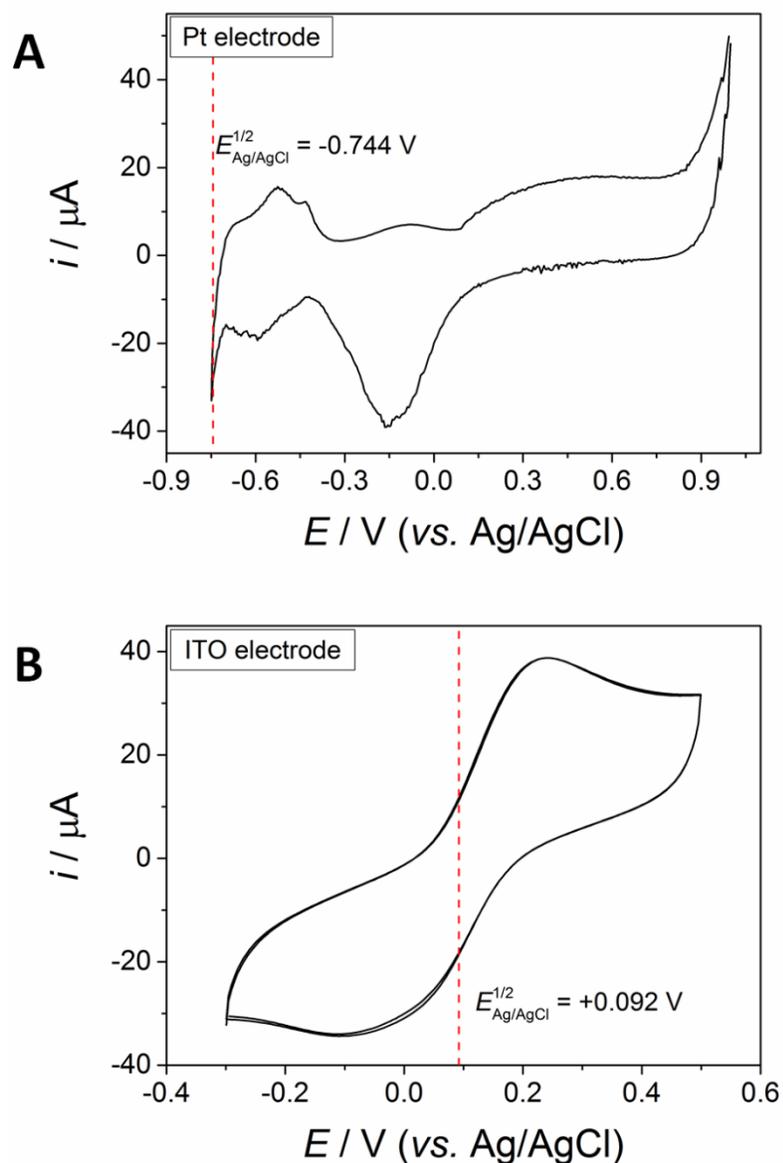
Fig. S1. (A) CV of phosphate buffer solution at pH 7 (degassed, and maintained under an inert N_2 atmosphere) *versus* the Ag/AgCl reference electrode. The working and counter electrodes were both Pt wire. The scan rate used was 20 mV·s^{-1}. **(B)** CV of an equimolar solution of $[Fe^{(III)}(CN)_6]^{3-}$ /$Fe^{(II)}(CN)_6]^{4-}$ in phosphate buffer solution, with a molar concentration of ~30 mM, at pH 7 *versus* the Ag/AgCl reference electrode. The working and counter electrodes were an ITO slide and Pt wire, respectively. The scan rate used was 20 mV·s^{-1}.

S.1.3   Electrochemical experiments at the interface between two immiscible electrolyte solutions (ITIES) to calibrate all voltammetry data obtained in the 4-electrode CBPEC configuration to the Galvani potential scale

Electrochemical measurements at the ITIES formed between an aqueous phosphate buffer solution and organic TFT solution, containing 5 mM BATB organic electrolyte, were performed using a 4-electrode electrochemical cell, as described previously [3]. In this 4-electrode configuration, the organic Pt and Ag/AgCl electrodes were connected to the counter and reference terminals, respectively, while the aqueous Pt and Ag/AgCl electrodes were connected to the working and sensing terminals, respectively. All experiments were carried out under aerobic conditions.

The applied potential (*E*) in the 4-electrode cell used to obtain CVs at the ITIES is defined as the potential difference established between the Ag/AgCl reference electrode in the aqueous phase and that in the organic reference solution. The applied potential (*E*) encompasses firstly the potential difference (or potential drop) that spans the interface between the aqueous and organic phases, known as the Galvani potential difference ($\Delta_o^w \phi$). The latter is defined as $\Delta_o^w \phi = (\phi^w - \phi^o)$, where ϕ^w and ϕ^o are the inner Galvani potentials of the aqueous and organic phases, respectively. Additionally, the applied potential (*E*) is determined by the nature of the reference electrodes used (for example a junction potential exists between the organic TFT solution and the organic reference solution). These contributions to the applied potential (*E*) are defined here as $\Delta E_{\text{ref.}}$. Thus, to calibrate the CVs at the ITIES to the Galvani potential scale the following relationship exists: $E = \Delta_o^w \phi + \Delta E_{\text{ref.}}$. The critical value of $\Delta E_{\text{ref.}}$ may be determined using the electrochemical response of model ion transfer probes, such as tetramethylammonium cations (TMA$^+$), at the ITIES in conjunction with the tetraphenylarsonium tetraphenylborate (TATB) assumption [4].

Previously, Olaya *et al.* precisely determined the half-wave potential of TMA$^+$ ion transfer at the ITIES formed between water and TFT ($\Delta_o^w \phi_{1/2}^{w \rightarrow \text{TFT}}(\text{TMA}^+)$) *versus* the origin of the Galvani potential scale as 0.270 V [4]. Using this value, the standard ion transfer potential of TMA$^+$ from water to TFT ($\Delta_o^w \phi_{\text{tr.}}^{\ominus, w \rightarrow \text{TFT}}(\text{TMA}^+)$) was determined to be 0.311 V. Thus, herein, TMA$^+$ was added to the aqueous phase and acted as a "secondary" reference ion for the calibration of the polarisable potential window to the Galvani potential scale using the following relationship

between the applied potential (E), the Galvani potential difference ($\Delta_o^w \phi$), the experimentally measured half-wave potential of TMA$^+$ ($E_{1/2}^{w \to TFT}(TMA^+)$) and the standard ion transfer potential of TMA$^+$ ($\Delta_o^w \phi_{tr.}^{\ominus,w \to TFT}(TMA^+)$):

$$\Delta_o^w \phi - \Delta_o^w \phi_{tr.}^{\ominus,w \to TFT}(TMA^+) = E - E_{1/2}^{w \to TFT}(TMA^+)$$

(S1)

$$E = \Delta_o^w \phi - \Delta_o^w \phi_{tr.}^{\ominus,w \to TFT}(TMA^+) + E_{1/2}^{w \to TFT}(TMA^+)$$

(S2)

$$E = \Delta_o^w \phi + [E_{1/2}^{w \to TFT}(TMA^+) - \Delta_o^w \phi_{tr.}^{\ominus,w \to TFT}(TMA^+)]$$

(S3)

$$E = \Delta_o^w \phi + \Delta E_{ref.}$$

(S4)

Herein, $E_{1/2}^{w \to TFT}(TMA^+)$ was measured as 0.780 V using our experimental setup at the ITIES (data not shown) and, thus, $\Delta E_{ref.}$ was determined as 0.469 V. As the reference electrodes used at the ITIES and the CBPEC configuration are identical, this value of $\Delta E_{ref.}$ was used to calibrate all voltammetry data obtained in the CBPEC configuration to the Galvani potential scale.

S.1.4   The current convention with a 4-electrode CBPEC

It is important to note that the peaks on the forward and reverse CV sweeps in a 4-electrode CBPEC indicate the progress of two half-reactions. In a conventional 3-electrode electrochemical cell, the peak on the forward sweep with a positive current simply means the species in solution is oxidised at that potential on the working electrode. However, in the 4-electrode CBPEC with aqueous-organic solutions, the peak on the forward sweep with a positive current indicates the flow of negative charge, *i.e.,* electrons, from the organic to aqueous compartment. Taking the half-reactions outlined in Equations (2) and (3) as an example, a positive current indicates the simultaneous reduction of Cyt c-Fe$_w^{(III)}$ to Cyt c-Fe$_w^{(II)}$ at P$_w$ and oxidation of DcMFc$_o^0$ to DcMFc$_o^+$ at P$_o$ on the forward sweep, scanning positively. When the sweep direction is reversed and scanned negatively, the back-reactions in Equations (2) and (3), main text, take place, and electrons flow from the aqueous to organic compartment giving rise to a negative peak.

6

S2   Voltammetry of Cyt *c* and the lipophilic electron donors in individual 3-electrode electrochemical cells

The redox potential of the Cyt *c*-Fe$^{(III)}$/Cyt *c*-Fe$^{(II)}$ redox couple in phosphate buffer solution at pH 7 *versus* SHE ($\left[E^{\ominus}_{\text{Cyt } c\text{-Fe}_w^{(III)}/\text{ Cyt } c\text{-Fe}_w^{(II)}}\right]^w_{\text{SHE}}$) was determined as +0.267 V using a 3-electrode cell, as described in section 2.1, with an ITO working electrode (Fig. S2(A)). This value is in excellent agreement with previous studies where $\left[E^{\ominus}_{\text{Cyt } c\text{-Fe}_w^{(III)}/\text{ Cyt } c\text{-Fe}_w^{(II)}}\right]^w_{\text{SHE}}$ for native Cyt *c* from bovine heart at pH 7 was determined as +0.263 V [5]. Using the Fc$^+$/Fc redox couple as an internal calibrant, the redox potential of the DcMFc$^+$/DcMFc redox couple in TFT *versus* SHE ($\left[E^{\ominus}_{\text{DcMFc}_o^+/\text{DcMFc}_o^0}\right]^o_{\text{SHE}}$) was determined as +0.107 V from a CV of a mixture of 10 µM Fc and 10 µM DcMFc in TFT with 5 mM BATB supporting electrolyte (Fig. S2(B), solid black line). Similarly, using DcMFc as the calibrant, the redox potential of the DiMFc$^+$/DiMFc redox couple in TFT *versus* SHE ($\left[E^{\ominus}_{\text{DiMFc}_o^+/\text{DiMFc}_o^0}\right]^o_{\text{SHE}}$) was determined as +0.584 V from a CV of a mixture of 10 µM DcMFc and 10 µM DiMFc in TFT with 5 mM BATB supporting electrolyte (Fig. S2(B), solid blue line).
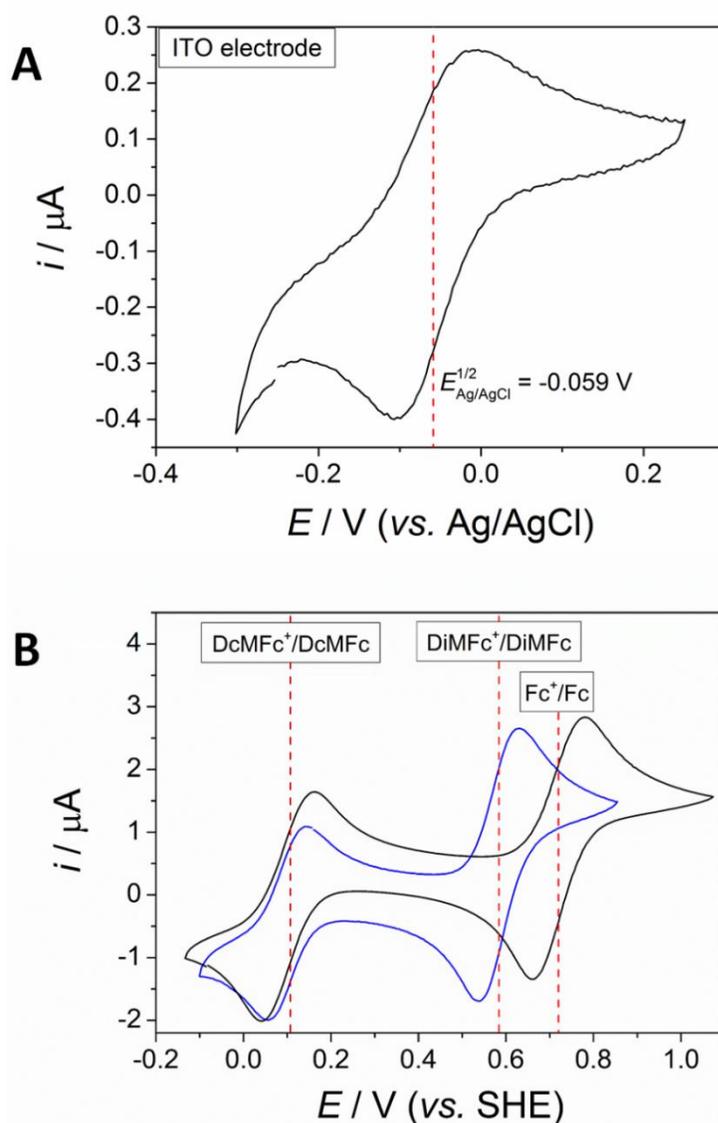
Fig. S2. **(A)** Cyclic voltammetry (CV) of 8 μM Cyt c in phosphate buffer solution at pH 7, with a molar concentration of ~2 mM, *versus* the Ag/AgCl reference electrode in a 3-electrode cell. The working and counter electrodes were an ITO slide and Pt wire, respectively. $\left[E^{1/2}_{\text{Cyt } c\text{-Fe}^{(\text{III})}_{\text{w}}/\text{ Cyt } c\text{-Fe}^{(\text{II})}_{\text{w}}}\right]^{\text{w}}_{\text{Ag/AgCl}} = -0.059 \text{ V}$ is equivalent to $\left[E^{\ominus}_{\text{Cyt } c\text{-Fe}^{(\text{III})}_{\text{w}}/\text{ Cyt } c\text{-Fe}^{(\text{II})}_{\text{w}}}\right]^{\text{w}}_{\text{SHE}} = +0.267 \text{ V}$, knowing $\Delta E^{\text{w}}_{\text{Ag/AgCl } vs. \text{ SHE}} = 0.326 \text{ V}$ (see section S1.2). The scan rate used was 20 mV·s^{-1}. **(B)** CVs of 10 μM Fc and 10 μM DcMFc (solid black line) and 10 μM DcMFc and 10 μM DiMFc (solid blue line) in TFT with 5 mM BATB supporting electrolyte. The working and counter electrodes were an ITO slide and Pt, respectively. The reference electrode, immersed in the organic reference solution, was a Ag/AgCl wire. The CVs were calibrated to the SHE scale using the known redox potential of the Fc$^+$/Fc redox couple *versus* SHE in TFT solvent as an internal calibrant. The scan rate used was 20 mV·s^{-1}.

S3   The sensitivity of ITO electrodes to electrochemical reduction

ITO is known to undergo morphological changes and dissolve on application of very negative cathodic potentials when used as the working electrode in a 3-electrode cell [6–8]. The electrochemical behaviour of ITO is highly dependent on the properties of the solution media, in particular the pH. Protons are known to be involved in the possible reduction reactions [7]:

$$In_2O_3 + 6H^+ + 6e^- \rightarrow 2In + 3H_2O$$

$$(S5)$$

$$SnO_2 + 4H^+ + 4e^- \rightarrow Sn^{2+} + 2H_2O$$

$$(S6)$$
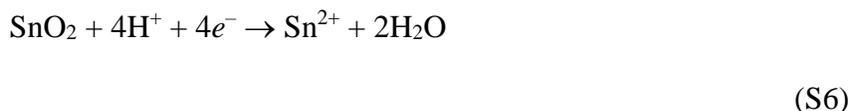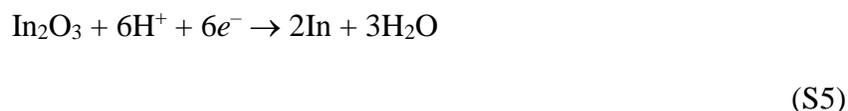
The electrochemical behaviour of ITO under the experimental conditions present in the aqueous compartment of the 4-electrode CBPEC (phosphate buffer solution at pH 7) was examined. Scanning to negative potentials, the onset of negative current was clearly observed at approximately –0.100 V *vs.* SHE (Fig. S3). This value is consistent with previous reports of SnO_2 reduction at +0.070 V *vs.* SHE in sulphuric acid at ~ pH 1 [8]. As expected, following the Nernst equation, a positive shift of the reduction potential occurs as the acidity increases since protons are involved (see Equations S5 and S6).
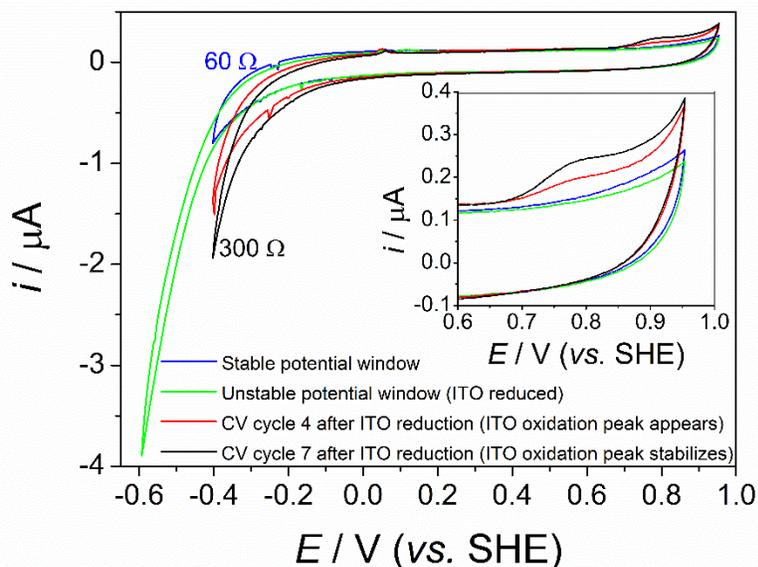
Fig. S3. Electrochemical reduction of ITO on application of very cathodic potentials. The ITO was the working electrode, with Pt and Ag/AgCl wires as the counter and reference electrodes, respectively. The aqueous solution consisted of phosphate buffer solution at pH 7. The scan rate used was 20 mV·s^{-1}. Inset: the appearance of oxidation peaks, attributed to the re-oxidation of metallic In or Sn, in CV cycles subsequent to extending the potential window negatively.

ITO may lose its conductivity and transparency under extreme anodic or cathodic polarisation [7]. Therefore, a straightforward experiment to evaluate the irreversibility of ITO reduction involved extending the polarisable potential window to very negative potentials during a CV cycle (*e.g.,* down to –0.600 V *vs.* SHE as shown in Fig. S3) and comparing the resistivity before and after negative bias. The resistivity was found to increase from 60 Ω to 200 Ω, clearly indicating ITO's loss of conductivity is permanent once the stable polarisable potential window has been exceeded cathodically. A further consequence of negative polarisation was the subsequent appearance of oxidation peaks in the anodic region, attributed to the re-oxidation of metallic In or Sn. Thus, attention must be paid to the positive and negative polarisation limits during a 4-electrode CPBEC experiment, in particular for the pole of the ITO BPE in the aqueous compartment.

S4   Calculations linking the aqueous Ag/AgCl reference electrode potential scale to the DcMFc potential scale in the TFT organic electrolyte

These calculations are rationalised as follows:

$$\Delta_o^w \phi = \left(\left[E_{\text{DcMFc}_o^+/\text{DcMFc}_o^0}^{1/2} \right]_{\text{Ag/AgCl}}^o + \Delta E_{\text{Ag/AgCl } vs. \text{ SHE}}^o \right)$$
$$- \left(\left[E_{\text{Cyt } c\text{-Fe}_w^{(III)}/\text{Cyt } c\text{-Fe}_w^{(II)}}^{1/2} \right]_{\text{Ag/AgCl}}^w + \Delta E_{\text{Ag/AgCl } vs. \text{ SHE}}^w \right)$$

$$(S7)$$

$$\Delta_o^w \phi = \left[E_{\text{DcMFc}_o^+/\text{DcMFc}_o^0}^{\ominus} \right]_{\text{SHE}}^o - \left(\left[E_{\text{Cyt } c\text{-Fe}_w^{(III)}/\text{Cyt } c\text{-Fe}_w^{(II)}}^{1/2} \right]_{\text{Ag/AgCl}}^w + \Delta E_{\text{Ag/AgCl } vs. \text{ SHE}}^w \right)$$

$$(S8)$$

$$\Delta_o^w \phi = - \left[E_{\text{Cyt } c\text{-Fe}_w^{(III)}/\text{Cyt } c\text{-Fe}_w^{(II)}}^{1/2} \right]_{\text{Ag/AgCl}}^w + \left(\left[E_{\text{DcMFc}_o^+/\text{DcMFc}_o^0}^{\ominus} \right]_{\text{SHE}}^o - \Delta E_{\text{Ag/AgCl } vs. \text{ SHE}}^w \right)$$

$$(S9)$$

$$\Delta_o^w \phi = \left(- \left[E^{1/2}_{\text{Cyt } c\text{-Fe}_w^{(III)}/ \text{Cyt } c\text{-Fe}_w^{(II)}}\right]^w_{\text{Ag/AgCl}} + \Delta_o^w \phi_{\text{Offset}}\right)$$

$$(S10)$$

The offset potential difference between the aqueous Ag/AgCl reference electrode and the SHE in a phosphate buffer solution at pH 7 ($\Delta E^w_{\text{Ag/AgCl } vs.\text{ SHE}}$) was 0.326 V. Since $\left[E^{\ominus}_{\text{DcMFc}_o^+/\text{DcMFc}_o^0}\right]^o_{\text{SHE}} = +0.107$ V, as shown in Fig. 2(B), SI, a net offset *versus* the interfacial Galvani potential difference ($\Delta_o^w \phi_{\text{Offset}}$) of –0.219 V was determined.

Supplementary References

[1] S. Trasatti, Pure Appl. Chem. 58 (1986) 955–966. doi:10.1351/pac198658070955.
[2] J.E. O'Reilly, Biochim. Biophys. Acta - Bioenerg. 292 (1973) 509–515. doi:10.1016/0005-2728(73)90001-7.
[3] E. Smirnov, P. Peljo, M.D. Scanlon, H.H. Girault, ACS Nano. 9 (2015) 6565–6575. doi:10.1021/acsnano.5b02547.
[4] A.J. Olaya, P. Ge, H.H. Girault, Electrochem. Commun. 19 (2012) 101–104. doi:10.1016/j.elecom.2012.03.010.
[5] G. Battistuzzi, M. Borsari, J.A. Cowan, A. Ranieri, M. Sola, J. Am. Chem. Soc. 124 (2002) 5315–5324. doi:10.1021/ja017479v.
[6] M. Senthilkumar, J. Mathiyarasu, J. Joseph, K.L.N. Phani, V. Yegnaraman, Mater. Chem. Phys. 108 (2008) 403–407. doi:10.1016/j.matchemphys.2007.10.030.
[7] L. Liu, S. Yellinek, I. Valdinger, A. Donval, D. Mandler, Electrochim. Acta. 176 (2015) 1374–1381. doi:10.1016/j.electacta.2015.07.129.
[8] S. Geiger, O. Kasian, A.M. Mingers, K.J.J. Mayrhofer, S. Cherevko, Sci. Rep. 7 (2017) 3–9. doi:10.1038/s41598-017-04079-9.